22. C. E. Kolb *et al.*, in *Progress and Problems in Atmospheric Chemistry*, J. R. Barker, Ed. (World Scientific, Singapore, 1995), vol. 3, pp. 771–875.
23. H. R. Pruppacher and R. Jaenicke, *Atmos. Environ.* **38**, 283 (1995).
24. T. E. Graedel and P. J. Crutzen, *Atmospheric Change: An Earth System Perspective* (W. H. Freeman, New York, 1993).
25. W. L. Chameides, *Geophys. Res.* **89**, 4739 (1984).
26. ______ and A. Stelson, *ibid.* **97**, 20565 (1992).
27. D. J. Hofmann, *ibid.* **98**, 12753 (1993).
28. R. J. Charlson *et al.*, *Science* **255**, 423 (1992).
29. J. T. Houghton *et al.*, *Climate Change 1995: The Science of Climate Change* (Cambridge University Press, Cambridge, 1996).
30. M. A. Tolbert, J. Pfaff, I. Jayaweera, M. J. Prather, *J. Geophys. Res.* **98**, 2957 (1993).
31. R. B. Chatfield, *Geophys. Res. Lett.* **21**, 2705 (1994).
32. J. J. Orlando, G. S. Tyndall, J. G. Calvert, *Atmos. Environ.* **26A**, 3111 (1992).
33. X. Li, H. Maring, D. Savoie, J. M. Prospero, *Nature* **380**, 416 (1996).
34. M. O. Andreae and P. J. Crutzen, *Science* **276**, 1052 (1997).
35. A. R. Chughtai, M. E. Brooks, D. M. Smith, *J. Geophys. Res.* **101**, 19505 (1996).
36. T. Novakov and J. E. Penner, *Nature* **365**, 823 (1993).
37. A. M. Middlebrook, D. M. Murphy, D. S. Thomson, in preparation.
38. C. A. Noble and K. A. Prather, *Environ. Sci. Technol.* **30**, 2667 (1996).
39. D. A. Hauglustaine, B. A. Ridley, S. Solomon, P. G. Hess, S. Madronich, *Geophys. Res. Lett.* **23**, 2609 (1996).
40. R.-S. Tseng, J. T. Viechnicki, R. A. Skop, J. W. Brown, *J. Geophys. Res.* **97**, 5201 (1992).
41. M. J. Rood, D. S. Covert, T. V. Larson, *Tellus* **39B**, 383 (1987).
42. B. J. Finlayson-Pitts, M. J. Ezell, J. N. Pitts, *Nature* **337**, 241 (1989).
43. R. Vogt, P. J. Crutzen, R. Sander, *ibid.* **383**, 327 (1996).
44. Y. Rudich, R. K. Talukdar, A. R. Ravishankara, in preparation.
45. L. A. Barrie, J. W. Bottenheim, R. C. Schnell, P. J. Crutzen, R. A. Rasmussen, *Nature* **334**, 138 (1988).
46. C. A. Rogaski, D. M. Golden, L. R. Williams, *Geophys. Res. Lett.* **24**, 381 (1997).
47. D. J. Lary *et al.*, *J. Geophys. Res.* **102**, 3671 (1997).
48. D. R. Hanson and A. R. Ravishankara, *J. Phys. Chem.* **98**, 5728 (1994).
49. P. V. Danckwerts, *Gas-Liquid Reactions* (McGraw-Hill, New York, 1970).
50. ______, *Trans. Faraday Soc.* **47**, 1014 (1951).
51. S. E. Schwartz, in *Chemistry of Multiphase Atmospheric Systems*, W. Jaenchke, Ed. (Springer-Verlag, Berlin, Heidelberg, Germany, 1986), vol. G6, pp. 415–471.
52. D. R. Hanson, A. R. Ravishankara, S. Solomon, *J. Geophys. Res.* **99**, 3615 (1994).
53. N. A. Fuchs and A. G. Sutugin, *Highly Dispersed Aerosols* (Ann Arbor Science, Ann Arbor, MI, 1970).
54. ______, in *Topics in Current Aerosol Research*, G. M. Hidy and J. C. Brock, Eds. (Pergamon, Oxford, 1971), pp. 1–60.
55. D. R. Hanson and E. R. Lovejoy, *Science* **267**, 1326 (1995).
56. E. R. Lovejoy and D. R. Hanson, *J. Phys. Chem.* **99**, 2080 (1995).
57. D. R. Haynes, N. J. Tro, S. M. George, *ibid.* **96**, 8502 (1992).
58. B. J. Gertner and J. T. Hynes, *Science* **271**, 1563 (1996).
59. M. Faraday, *Philos. Mag.* **17**, 162 (1859).
60. P. V. Hobbs, *Ice Physics* (Clarendon, Oxford, 1974).
61. M. Elbaum, S. G. Lipson, J. G. Dash, *J. Cryst. Growth* **129**, 491 (1993).
62. Y. Mizuno and N. Hanafusa, *J. Phys. Colloq. C1* **48**, (suppl. 3), C1-511 (1987).
63. N. Materer *et al.*, *J. Phys. Chem.* **99**, 6267 (1995).
64. G. P. Gervat *et al.*, *Nature* **333**, 241 (1988).
65. A. S. Chandler *et al.*, *ibid.* **336**, 562 (1988).
66. R. W. Johnston and G. E. Gordon, Eds., *The Chemistry of Acid Rain: Sources and Atmospheric Processes* (American Chemical Society, Washington, DC, 1987), vol. 349.
67. Y. Rudich, R. K. Talukdar, T. Imamura, R. W. Fox, A. R. Ravishankara, *Chem. Phys. Lett.* **261**, 467 (1996).
68. Y. Rudich, R. K. Talukdar, A. R. Ravishankara, R. W. Fox, *J. Geophys. Res.* **101**, 21023 (1996).
69. T. Imamura, Y. Rudich, R. K. Talukdar, R. W. Fox, A. R. Ravishankara, *J. Phys. Chem.* **101**, 2316 (1997).
70. B. J. Finlayson-Pitts and J. N. Pitts, *Atmospheric Chemistry: Fundamentals and Experimental Techniques* (Wiley, New York, 1986).
71. P. W. Villalta, E. R. Lovejoy, D. R. Hanson, *Geophys. Res. Lett.* **23**, 1765 (1996).

72. I am most grateful to my colleagues D. Hanson, S. Solomon, R. Talukdar, Y. Rudich, T. Imamura, E. Lovejoy, C. Howard, R. Utter, and J. Burkholder for helping me explore the "heterogeneous" world. I thank S. Madronich, S. George, D. Hofmann, G. Feingold, J. Lelieveld, A. Middlebrook, D. Murphy, B. Finlayson-Pitts, J. Pitts Jr., M. O. Andreae, P. Crutzen, and an anonymous referee for helpful discussions, suggestion, preprints, and references. I thank many of my aeronomy laboratory colleagues for comments on this review. I am indebted to P. Crutzen for many stimulating discussions over the past decade which made me think about this issue. Funded in part by NOAA's Climate and Global Change Research Program.

Measurement Techniques in Gas-Phase Tropospheric Chemistry: A Selective View of the Past, Present, and Future

Howard K. Roscoe* and Kevin C. Clemitshaw

Measurements of trace gases and photolysis rates in the troposphere are essential for understanding photochemical smog and global environmental change. Chemical measurement techniques have progressed enormously since the first regular observations of tropospheric ozone in the 19th century. In contrast, by the 1940s spectroscopic measurements were already of a quality that would have allowed the use of modern analysis techniques to reduce interference between gases, although such techniques were not applied at the time. Today, chemical and spectroscopic techniques complement each other on a wide range of platforms. The boundaries between spectroscopic techniques will retreat as more Fourier transform spectrometers are used at visible wavelengths and as wide-band lidars are extended, and combining chemical techniques will allow detection of more trace gases with better sensitivity. Other future developments will focus on smaller, lighter instruments to take advantage of new platforms such as unmanned aircraft and to improve the effectiveness of urban sampling.

Modern tropospheric chemistry is the study of oxidants (O_3, OH, H_2O_2, HCHO, HO_2, and NO_3), gases that can be oxidized (hydrocarbons and sulfur compounds), oxidation products (carbonyls and organic nitrates), and the interactions of all of these with aerosols and clouds. Tropospheric chemistry is receiving particular attention today because of the widespread occurrence of photochemical smog in the Northern Hemisphere, which is often observable at considerable distances from the sources of pollutants. Effective pollution abatement strategies must be based on a detailed understanding of the causes and effects of pollution. We must be able to predict the three-dimensional evolution of the chemical composition of the troposphere, on spatial scales from the urban to the regional and eventually to the global. In order to define the initial state of the system and to validate model predictions, measurements must be made on each of these spatial scales. Tropospheric chemistry also presents different challenges and issues according to geographical location and altitude. These challenges have been met by deploying a wide range of instruments on different platforms. The limitations of these platforms have influenced sensor design in the past and will do so more vigorously in the future. There is a wide range of techniques for measuring tropospheric trace gases in ways that are appropriate to the different spatial scales. Because of their substantially different heritages, we make a broad distinction between spectroscopic absorption techniques, which observe over horizontal path lengths of 3 to 10 km or in a cell with mirrors to fold the path, and more localized chemical techniques, although this distinction is blurred in

---

H. K. Roscoe, British Antarctic Survey/Natural Environment Research Council, Madingley Road, Cambridge CB3 0ET, UK.
K. C. Clemitshaw, Centre for Environmental Technology, Imperial College of Science, Technology and Medicine, Silwood Park, Ascot SL5 7PY, UK.

*To whom correspondence should be addressed.

the case of spectroscopic sensors, which stimulate fluorescence from a small volume of gas. The spectroscopic techniques can observe over sufficiently short path lengths to be applied to the urban scale, so the distinction from chemical techniques is one of heritage rather than of applicability. Because photolysis initiates much of the chemistry of oxidants, it is also important to measure the photolysis rates of trace gases. Techniques for measuring photolysis rates share much of a common heritage with techniques for gas-phase measurements.

Here we present a selective review of techniques for measuring tropospheric trace gases and photolysis rates and give our view of future directions. Although we recognize their importance in improving models and defining their boundary conditions, lack of space forbids discussion of measurements of fluxes of trace gases. Similarly, measurements of aerosol and cloud chemistry, which are important for global tropospheric chemistry (though less so for photochemical smog), are also omitted. Their techniques differ substantially from those of gas-phase measurements and are a major subject in themselves. Some recent reviews deal less selectively with measurement techniques (*1*, *2*).

The Past

The earliest tropospheric oxidant to be measured was ozone (O_3), which was routinely observed at over 300 sites in Europe and the United States between 1850 and the early 1900s. This massive interest was stimulated by the supposed ability of O_3 to reduce epidemics, particularly of cholera, and by its general association with health, an idea now known to be mistaken, because O_3 is toxic. The measurement technique, pioneered by Schonbein, used papers covered in a paste of starch and KI, which is turned blue by O_3. After 12 hours of exposure, the amount of O_3 was deduced by comparison with colors on a test chart. These "Schonbein papers" were also affected by other oxidants and by humidity and sunlight, but a quantitative revision of the data from many sites has been possible (*3*) because of simultaneous measurements of O_3 with Shonbein papers and a more discriminating method using arsenic potash at Montsouris Observatory near Paris, beginning in 1876. This comprehensive revision concluded that the average amount of surface O_3 in Michigan in the late 19th century was between about 16 and 20 parts per billion by volume (ppbv), which is much less than today. Similarly small values were found at Montsouris when the more reliable technique was used.

By 1912, absorption of ultraviolet (UV) light was being used to measure O_3 in the laboratory (*4*). Because extinction (scattering) by air molecules is proportional to wavelength^{-4}, extinction is greater in the UV than in the visible. Despite the difficulty this creates for atmospheric UV measurements, Strutt (*5*) concluded that there was less than 27 m atm cm of O_3 in a 4-mile path at night (42 ppbv); our own estimate by eye from his photographic plates suggests 20 ppbv, which is consistent with the Montsouris measurements. By 1934, classical spectroscopic measurements had improved to the excellent quality of the spectrum of O_2 (*6*) reproduced in Fig. 1. Measurements of this quality would be considered outstanding even today. They have better spectral resolution than some current spectrometers that are in routine use for wide-bandwidth tropospheric measurements, because the grain size of film is much smaller than the pixels of modern array detectors, although their overall sizes are comparable.

A similarly high quality was achieved in infrared (IR) spectroscopy by the 1940s. IR spectra of the sun at 1 cm^{-1} resolution were used by Adel to identify atmospheric N_2O (*7*) and by Migeotte to identify atmospheric CH_4 (*8*). These workers were concerned with identification rather than with quantitative measurements—it is typical that Adel's comprehensive atlas of the solar IR spectrum (*9*) did not list solar angles. However, spectral quality was quite sufficient for quantitative determinations, and we were able to make a simple correlation with N_2O spectra (*7*) by eye. This gave the expected 0.3 parts per million (ppm) if the sun was at 45°. By 1949, rivalry between Adel in Arizona and Migeotte in Ohio led to conflicting claims about absorption by CO at 4.7 μm (*10*, *11*), which would now be ascribed to industrial Ohio versus clean Arizona.

These earliest spectroscopic measurements in the UV and IR were not analyzed quantitatively; this was no doubt partly because of the lack of computers, but there seem to have been no attempts at analysis by hand. It seems that the ideas behind least-squares fits were absent. However, we must emphasize that the spectra were of excellent quality, clearly sufficient for modern line-by-line and differential optical absorption spectroscopy (DOAS) analysis.

After the rapid development of electronic devices in the early 1940s, photomultiplier tubes replaced film as detectors. Because each tube could only detect a single wavelength at any one time, signals were often detected at only two wavelengths. Later, more wavelengths were added by correlation spectroscopy, in which a photographic replica of the inverse of the spectrum of the gas of interest replaced the exit slit (NO_2, SO_2, and CO were measured by commercial instruments). Gas-correlation spectroscopy worked on similar principles, but instead of a grating, a cell filled with the gas of interest and an empty cell were used to obtain the inverse function (*12*). These techniques increased the signal and reduced interference between gases, but were limited to the target gases; information about other gases was lost. Although many useful measurements were made by such specialized instruments, resources might have been better directed at improving and deploying wide-band instruments. For example, in the 1950s, Migeotte measured solar spectra from the Jungfraujoch at 3580 m in the Swiss Alps, enabling the amount of CH_4 in the atmosphere to be deduced (*13*); reanalysis of these and more recent spectra enabled Ehhalt *et al.* to deduce the trend in CH_4 and in C_2H_6 (*14*), illustrating the

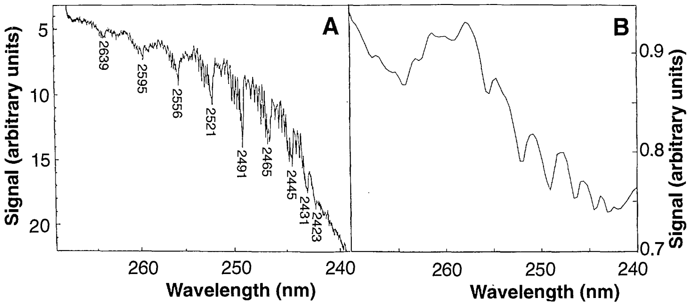

Fig. 1. (**A**) UV absorption spectrum of oxygen measured at night on the glacier below the Jungfraujoch observatory in 1933, from a hydrogen lamp at the observatory (*6*), measured to enable the bands of oxygen to be assigned. After developing the photographic plates of these spectra, they were analyzed by a microphotometer, so that signals were in electrical form (reproduced courtesy of *Revue d'Optique*, Masson Editeur). (**B**) UV part of the absorption spectrum from a modern instrument routinely used for tropospheric measurements by DOAS analysis (courtesy of J.-P. Pommereau and F. Goutail), relative to a quadratic line to compensate for wavelength dependence of its xenon lamp and so simplify the plot. The resolution of the modern spectrum is limited by the array detector if a wide bandwidth is to be achieved (see text), but it is quite sufficient for measurements of most tropospheric absorbers, as shown in Fig. 2B. Comparison between the spectra shows that the quality of the 1933 spectra would have been more than sufficient for modern DOAS analysis, if computers had been available for the analysis.

importance of wide-band spectral measurements, whereby advanced analysis techniques can be applied many years after the measurement was made. Unfortunately, no comparable open-path UV-visible measurements were made that might now allow us to deduce the amounts of, say, tropospheric NO_3 in the 1950s.

Present Spectroscopic Techniques

When compared to the classical spectroscopic techniques for tropospheric chemistry described above, the major improvements in today's sensors stem from the development of analytic techniques for the quantification of trace gas amounts in absorption spectra, and from the development of lasers as active IR and visible sources. Of these analytic techniques, DOAS (*2*) is of overwhelming importance, and we discuss it here in detail. We then review the active techniques that are currently in use and show how they are related or are becoming related to DOAS.

In the usual implementation of a system that uses DOAS analysis, a lamp illuminates a spectrometer and detector, which measures the absorption by the atmosphere between the lamp and the spectrometer. This absorption is analyzed to determine the amounts of trace gases in the atmosphere. DOAS is an analysis technique in which first, the spectrum is divided by the spectrum of the lamp with no atmospheric path, to derive the spectrum of the optical depth; second, a high-pass filter in wavelength space is applied to the spectrum of the optical depth; and finally, cross-sections of gases are least-squares fitted to this optical depth to determine their amounts. In the usual filter implementation, the difference between the measured optical depth and the same spectrum after smoothing is taken, and therefore the filtered optical depth is commonly called the differential optical depth. It is immune to details of molecular and aerosol scattering and to the spectral shape and calibration constants of the lamp and spectrometer.

If these spectral shapes are smooth, as for a tungsten rather than a xenon arc lamp, the spectrum of the lamp without atmosphere need not be measured. This is particularly important if the lamp is a broadband laser, because the measurement without atmosphere must necessarily be made in the near field of the laser, where the sample may have a different spectral response than in the far field after passage through the atmosphere (*15*). In some measurements of OH (*16*, *17*), this problem is elegantly avoided by using a laser with pulses of picosecond duration, resulting in a smooth spectrum because of the uncertainty principle. The pulse frequencies are sufficiently high that the detector cannot observe individual pulses, so that the signal appears continuous.

We must emphasize that DOAS is an analysis technique, which takes place in the computer after measurement. DOAS is not specific to instrumental details such as the type of detector, spectrometer, or lamp. Modern systems use detectors with many elements (array detectors) to observe the whole spectrum simultaneously; this was also achieved by film in some of the earliest implementations using DOAS analysis (*16*), but other early DOAS results were produced by scanning the spectrum, using a single photomultiplier as a detector (*17*, *18*). Measurements by DOAS analysis have even used lamps with very different spectral characteristics [xenon (*19*) and tungsten (*20*)] for the same gas (NO_3) at the same wavelength (662 nm). DOAS is also not specific to the path of the observation: Usually, a long open path with a nearby lamp

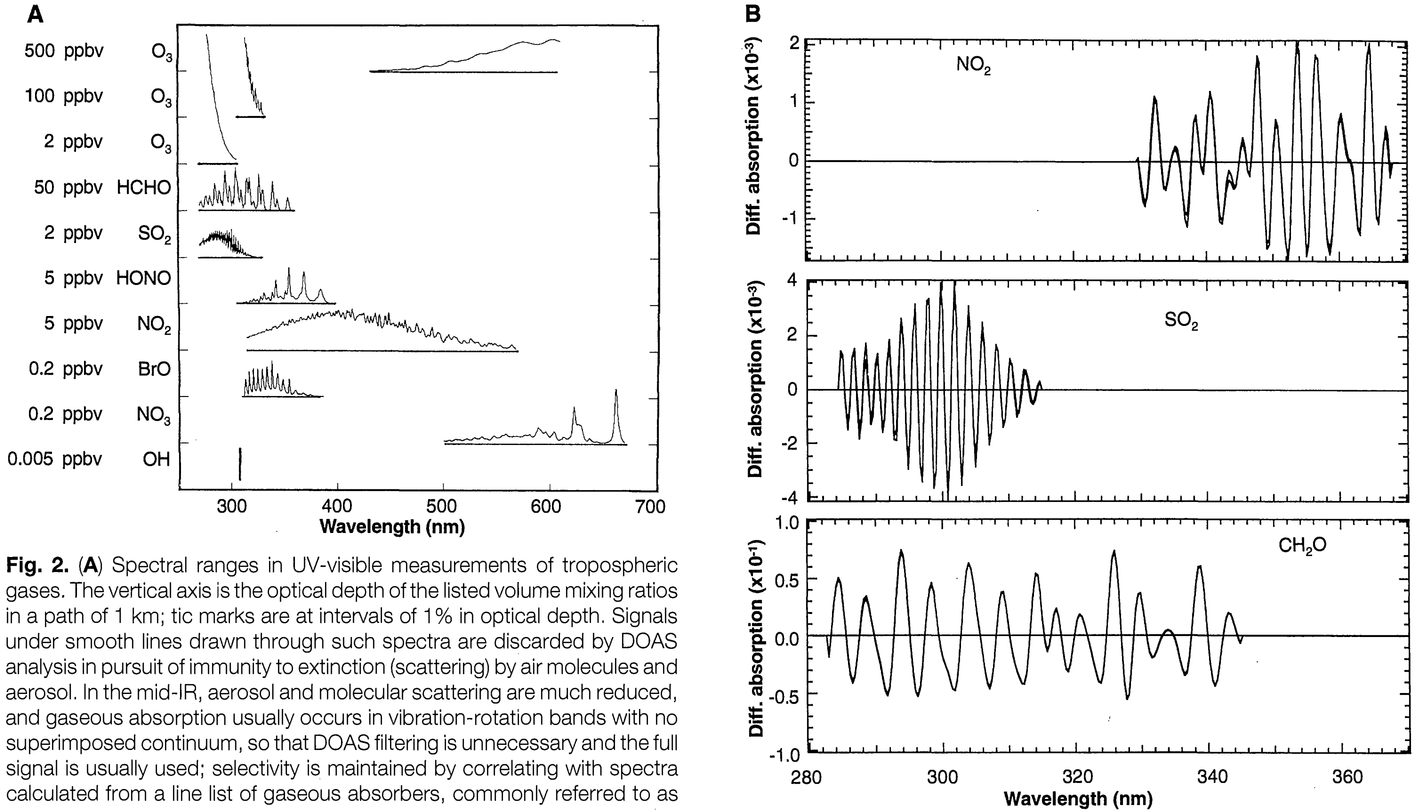

Fig. 2. (**A**) Spectral ranges in UV-visible measurements of tropospheric gases. The vertical axis is the optical depth of the listed volume mixing ratios in a path of 1 km; tic marks are at intervals of 1% in optical depth. Signals under smooth lines drawn through such spectra are discarded by DOAS analysis in pursuit of immunity to extinction (scattering) by air molecules and aerosol. In the mid-IR, aerosol and molecular scattering are much reduced, and gaseous absorption usually occurs in vibration-rotation bands with no superimposed continuum, so that DOAS filtering is unnecessary and the full signal is usually used; selectivity is maintained by correlating with spectra calculated from a line list of gaseous absorbers, commonly referred to as line-by-line analysis. (**B**) Differential optical depths (that is, after DOAS filtering) of part of a spectrum from a modern wide-band instrument (a different part of the raw spectrum is shown in Fig. 1B). Each plot shows two lines: the measured optical depths after subtraction of calculated optical depths due to other absorbers, and the optical depths calculated from the least-squares fit to laboratory cross-sections (courtesy of J.-P. Pommereau and F. Goutail). Agreement between measurements and fits is excellent, often better than 10^{-4} in optical depth.

and a distant retroreflector (*15*) is used, but a distant lamp or a shorter open cell with mirrors for mutiple relections of the beam (*21*) (commonly called a multipass cell) or a closed multipass cell can also be used.

In all but the most stable of spectrometers, the wavelengths at which the detector samples the spectrum of the lamp with and without atmosphere are not identical, so that one spectrum must be interpolated onto the sampling grid of the other before division. Interpolation errors then force a compromise between sampling ratio and bandwidth (*22*), so that with wide-bandwidth instruments minimum detectable amounts are compromised in favor of measuring more constituents, which is appropriate in polluted atmospheres with larger amounts of absorbers. Pommereau and coworkers increased bandwidths to cover the range from 250 to 500 nm (*23*), so that O_3, NO_2, SO_2, H_2O, and various hydrocarbons could be observed simultaneously (Fig. 2) by using an array detector that observed the whole spectrum simultaneously—a single detector that scanned over such a wide bandwidth would observe each wavelength too briefly, resulting in a worse signal-to-noise ratio (*24*). By contrast, bandwidth was sacrificed for better signal-to-noise ratio in DOAS measurements of OH at 308 nm (*15–17*). Because all available OH lines occupy less than 1 nm, a laser source can be used, which improves the power in the useful bandwidth.

In the IR, there are few array detectors because semiconductors other than Si have to be used at these longer wavelengths. Hence, tunable-diode laser (TDL) systems are favored over broad-band lamps. Noise in IR detectors is less at higher frequencies, so that frequency modulation or a high-speed sweep of the TDL is used to reduce noise. Modulation supplies high-pass filtering; such a modulated system can be understood as a DOAS system except that filtering takes place within the instrument instead of the computer. This method is less flexible than conventional DOAS because alternative filters cannot be tested after the measurement has been made. In contrast, a high-speed sweep allows a post-measurement choice of DOAS or non-DOAS analysis.

Many TDL systems favor multipass cells over long open paths, so that the pressure of the sample can be reduced, thereby narrowing the pressure-broadened lines and increasing the selectivity for each absorber. When systems are operated at ambient pressure, multipass cells are still favored because modulation may coincide with fluctuations in the atmosphere. An innovative way of avoiding modulation while using a long open path was adopted by the light detection and ranging (lidar) method at Stanford (*25*) before eye safety became an issue. The target was topographic (a building or hill), and by sweeping the tunable IR oscillator and analyzing simultaneously for CO_2 and H_2O, the DOAS principle was maintained (*26*).

In the mid-IR, extinction by air molecules is smaller (the wavelength is larger), so there is no advantage from DOAS analysis. Fitting to the full rather than the filtered spectrum allows one to observe a greater absorption signal (this would also be true in the visible, as can be seen by inspection of Fig. 2). Such line-by-line fits are widely used when determining the total tropospheric column of an absorber from solar spectra, where IR measurements have another advantage over the visible: In the visible, absorption by the sun's atmosphere (Fraunhofer lines) interferes so that the ratio of high to low sun must be measured, whereas in the IR, the solar lines can be distinguished within one spectrum because of their higher temperatures and resulting greater width. Only modest spectral resolution is needed, because lines are pressure-broadened to about 0.1 cm^{-1} at 1 atm. With a resolution of 0.01 cm^{-1}, a vertical profile with resolution of 5 to 7 km can be retrieved in the troposphere. A Fourier transform spectrometer (FTS) is usually used, whereby the whole spectrum can be measured simultaneously. The compact FTS is now also used in IR measurements with a lamp as source. Simultaneous measurements of CO, CH_4, and N_2O can be made with excellent precision (*27*), and an airborne FTS has made measurements from 2650 to 600 cm^{-1} with a resolution of 0.36 cm^{-1} (*28*). A small bench-top FTS can now measure wavelengths from 15,000 to 30 cm^{-1} with a resolution of 0.15 cm^{-1}.

Progress in measurements by lidar has followed that of measurements with continuous light sources. In lidar, a short pulse of light is emitted upward, and light from the pulse that is scattered downward by the atmosphere is detected as a function of time after the pulse. The time is proportional to the distance traveled by the light, so that one can deduce the vertical profile of the product of the density of the scatterer times the absorption between the source and the scatterer. In the late 1960s, lidars were single-wavelength and were used to measure aerosols. Later, dual-wavelength lidars, termed differential absorption by lidar (DIAL), measured O_3 in the UV (*29*, *30*), and more wavelengths were added to measure more gases (*26*). Conventional analysis uses the DIAL equation, whereby ratios of signals at successive ranges cancel atmospheric scattering and instrument functions, but this relies on total overlap of output beam by the receiver and on lack of discontinuity in aerosol scattering (no thin clouds). Recently, broad-band lasers have been combined with classic DOAS analysis to measure H_2O (*31*): This innovative and powerful analysis technique is still valid when thin clouds are present and with partial beam overlap.

Present Chemical Sensors

Many chemical sensors measure tropospheric trace gases that cannot be measured by spectroscopic sensors. When the same gas can be measured with the use of either approach, they can have very different sources of error. If so, then intercomparison can improve confidence in the accuracy or in the detection limit claimed by either.

Chemical sensors may be considered in several groups. Chromatographs separate trace gases that are present in ambient or preconcentrated air in a capillary, after which the gases are detected in a variety of ways, often with selectivity regarding types of compounds. Chemiluminescent sensors observe light emitted at specific wavelengths from the reaction of the desired gas with another gas or liquid. Peroxy radicals can be measured by chemical amplification, whereby NO and CO are catalytically converted to NO_2 and CO_2 via cycling between OH and HO_2. Peroxy, peroxy acetyl, NO_3, and other radicals can also be isolated in a matrix of D_2O-ice formed at cryogenic temperatures, followed by analysis of the matrix by electron spin-resonance spectroscopy. OH and HO_2 radicals can be measured by fluorescence assay with gas expansion (FAGE), whereby air is expanded through a nozzle to lower pressure (1 mbar), so that the fluorescence lifetime of the radical is increased; this allows a longer delay between the input light pulse and the fluorescence measurement, discriminating against light from the input pulse. High-pressure liquid chromatography (HPLC) with ion chromatography is a versatile and sensitive technique for the analysis of ions (NO_2^-, NO_3^-, NH_4^+, SO_4^{2-}, and acetate ions) and of organic compounds (carbonyls and polyaromatic hydrocarbons). Finally, OH radicals and other gases can be measured in mass spectrometers, often involving chemical ionization. Many of these techniques focus on measuring HO_2 and peroxy radicals because they play important parts in the production and loss of O_3 in the troposphere, form secondary pollutants such as peroxides and organic nitrates, and affect the formation of OH and the decomposition of peroxy-acetyl nitrate (PAN) at night (*32–34*).

In a gas chromatograph (GC), a variety of detection methods may be used (Table 1). Samples may be automatically analyzed in situ, with the use of programmed temperature vaporization injection (*35*), or collected in electropolished canisters filled to high pressures with pumps or cryogens. The samples are then analyzed in the laboratory by means of cryogenic preconcentration, with separation being achieved in wide-bore, porous-layer, open tubular columns of fused-silica, deactivated with Al_2O_3 and KCl (*36*). When the chromatograph is followed by a mass spectrometer, it provides unique fingerprints of the separated products. This is an extremely powerful method for detecting trace gases in the troposphere.

Commonly used chemiluminescent reactions are (i) the reaction of NO_2 in ambient air with luminol (5-amino-2,3-dihydro-1,4-phthalazinedione), which emits blue light (*37*), although its nonlinear response caused difficulties until recently, when it was established to be quadratic at small concentrations (*38*) and linear above 3 ppbv (*39*); and (ii) the reaction of NO in ambient air with O_3, which emits red light (*40*, *41*), a highly sensitive and selective technique for measuring NO. The latter reaction is also used as the detector in instruments that measure other nitrogen gases by converting them to NO:

(i) NO_2 is converted by exposure to UV light from a xenon lamp (*42*), whose wavelength coverage is ideal for minimizing interference from the photolysis of HONO or $RONO_2$; interference from the thermal decomposition of PAN and HO_2NO_2 to NO_2 is also minimized. Simultaneous measurements of NO and NO_2 may be made with two channels, each cycling through a sequence of NO, NO_2, and chemical zero (obtained by prereacting the sample air with O_3). Sensitivity approaches 10 counts s^{-1} $pptv^{-1}$ (pptv, parts per trillion by volume), with detection limits better than 1 pptv.

(ii) Total reactive nitrogen (the sum of NO, NO_2, NO_3, $2 \times N_2O_5$, HONO, $HONO_2$, HO_2NO_2, PAN, organic nitrates, and particulate nitrate), often referred to as NO_y, is converted to NO on gold above 300°C in the presence of 0.2% CO (*43*, *44*). Recent intercomparisons (*45*) have stimulated work on understanding the detailed mechanism of conversion and quantifying potential interferences from ambient HCN, NH_3, and H_2O. Note that commercial chemiluminescent instruments for NO_2 that use thermal molybdenum converters are not selective, as most other components of reactive nitrogen contribute to the NO_2 signal.

Chemical amplification of HO_2 and RO_2 radicals was proposed in the 1980s (*46*) and implemented by 1991 (*47*). The amplification factor must be measured by careful calibration. Many peroxy (RO_2) radicals, which collectively may be present in the troposphere at a concentration comparable to that of HO_2 (*48*), are efficiently converted to HO_2 in the presence of NO. Uncertainties in the technique are also associated with radical loss within the inlet system, with calibration, and with corrections for interferences by PAN and H_2O_2. Many of these uncertainties were recently addressed in two blind intercomparisons between measurements of ambient peroxy radicals (*49*) and of laboratory calibration sources of HO_2, CH_3O_2, and $CH_3C(O)O_2$ (*50*). It was found that the chemical amplifier and the matrix isolation and electron spin resonance (MIESR) techniques detect different subsets of the peroxy radical population present in the continental boundary layer; the former measures HO_2 and the fraction of RO_2 that upon reaction with NO is transformed into HO_2, whereas the latter detects HO_2 and all RO_2 by their spectroscopic signatures.

Measurements of peroxy radicals using MIESR were first reported by Mihelcic *et al.* (*51*). MIESR possesses the unique ability to measure simultaneously HO_2, $CH_3C(O)O_2$, the sum of alkyl peroxy radicals, NO_2, and NO_3. The first simultaneous observations of peroxy and NO_3 radicals in the troposphere (*52*) and measurements of ratios of HO_2 to RO_2 (*48*) were made using MIESR. The detection limit for peroxy radicals and NO_2 is 3 pptv; because of its narrower electronic spin resonance line width, it is 1 pptv for NO_3.

FAGE was pioneered by Hard and O'Brien in the 1980s (*53*). In more recent FAGE implementations by other workers, OH is detected by laser-induced fluorescence (LIF) at 308 nm, using a high-rate dye laser pumped by a copper-vapor laser, with detection limits of 10^6 molecules cm^{-3} in 1 min. Comparisons of recent FAGE implementations with other OH measurement techniques showed good agreement, confirming the absence of significant interferences or artifacts (*54*, *55*); LIF sensors have been criticized for their potential for creating OH via production of atomic oxygen by the laser light, followed by reaction with ambient H_2O, but recent studies using C_3F_6 to quench ambient OH demonstrated that the laser creates less than 5×10^{-3} ppt of OH (*56*). HO_2 can also be measured by FAGE, by converting to OH via reaction with NO, which is injected immediately after the nozzle; tropospheric amounts of HO_2 are typically 100 times larger than OH, so that very precise measurements of HO_2 may be made with instrumentation designed for detection of OH.

Finally, mass spectrometers combined with chemical ionization or ion molecule reaction techniques have recently achieved spectacularly small detection limits, measuring OH (*57*, *58*) and HO_2 and RO_2 radicals (*59*, *60*). In the latter case, a novel variation on the chemical amplification theme is used: HO_2 and RO_2 are converted with NO and O_2 to OH, which is then reacted with SO_2 in the presence of O_2 to produce SO_3 and regenerate HO_2 in a chain reaction. Chain termination occurs by reaction of SO_3 with water vapor to produce H_2SO_4, which is then detected after reaction with NO_3^- HNO_3 ions. OH measurements are accomplished in an identical manner but without the addition of NO. The method has also been used to detect H_2SO_4, HNO_3, HONO, dimethyl sulfide, and methane sulfonic acid, as reviewed recently (*61*).

Present Photolysis-Rate Sensors

Photolysis reactions are responsible for the production of many radicals that drive tropospheric chemistry: Photolysis of O_3 leads to formation of $O(^1D)$ atoms, which then react with water vapor to form OH; of NO_2 to $O(^3P)$ atoms, which react with O_2 to form O_3; of HONO to OH; and of HCHO to H atoms, which produce HO_2.

Direct measurements of photolysis rates require a reaction vessel that is illuminated with full ambient sunlight, both direct and diffuse. This is difficult to achieve without the reaction vessel being outdoors. The measurements themselves are extremely challenging even in the laboratory or on board a large aircraft, and much more so under in situ conditions. It is also very difficult to ensure representative solar illumination indoors or inside an airplane. Instruments may be very complex, requiring a well-characterized calibration source, a carefully constructed photolysis cell, and a

Table 1. Detection systems for gas chromatographs.

Detector	Trace gases measured
Flame ionization	Hydrocarbons and oxygenated hydrocarbons, C1 to C9; anthropogenic and biogenic
Electron capture	Chlorofluorocarbons and N_2O (*72*), PAN (*73*), alkyl nitrates (*74*)
React with reducer sense products	CO (with HgO at 265°C to Hg vapor, measured by UV photometer; limit, 1 ppbv
Mass spectrometer	Many, including hydrofluorocarbons and brominated hydrocarbons

fast response detector assembly (*62*, *63*). Another difficulty is that the integration time for high accuracy is often too long to be useful in measurements from aircraft, where the scene changes rapidly. Because of these difficulties, few such chemical actinometers have been developed to date.

Alternatively, the photolysis rate can be calculated from other measured quantities. The photolysis rate is the product of the solar flux, the absorption cross-section, and the quantum yield, integrated over wavelength and solid angle. Of these terms, cross-sections and yields can be measured in the laboratory, so it is sufficient to measure the flux, which depends on solar zenith angle, to determine the photolysis rate. Ideally, solar flux is measured by a spectroradiometer at a variety of angles, and the integrations are performed in the analysis computer. If the wavelength coverage is wide, fluxes for several gases are measured simultaneously. Alternatively, the angular integration can be made in the instrument either by using full spherical optics or, if corrections for varying albedo must be made, by using separate upward and downward hemispheric optics.

One can approximate both the wavelength and angular integrations by using a filter radiometer that views the whole sky. Such radiometers have good signal-to-noise ratios and are inexpensive and compact (*64*), but require accurate knowledge of the wavelength dependence of flux, cross-section, and quantum yield, whose product depends on solar zenith angle, so that a calibration against a chemical actinometer may be necessary. Despite these complications, a recent airborne instrument to measure the photolysis rate of NO_2 [$j(NO_2)$] produced results with excellent accuracy (*65*). Other commercially available radiometers to determine $j(NO_2)$ are based on the device described by Junkerman *et al.* (*64*), but using quartz diffusers to minimize dependence on the incident angle. They are accurate to 5% but must be calibrated annually against a chemical actinometer.

Present and Future Platforms

The most intensively studied part of the troposphere has traditionally been the boundary layer, because of the relative ease of measurements near the ground and because trace gases there have obvious effects on humans. Today, ground-based instruments are supplemented by instruments on aircraft, ships, and tethered balloons in the boundary layer (Fig. 3). Spectroscopic instruments have usually remained on the ground and used long open paths, but in the future the same instrument will routinely switch between a multipass cell and an open path, as pioneered by Galle *et al.* (*27*), who measured fluxes as well as concentrations with a single FTS by alternating the observed optical path between a multipass cell in ambient air, an open path, and air pumped from a tower. In the boundary layer, urban pollution is now a major issue, but three-dimensional measurements in cities are currently confined to towers because of safety issues regarding aircraft and large tethered balloons and because small balloons can only lift a few kilograms. Medium-sized tethered balloons (*66*) may pave the way to more comprehensive urban measurements.

The chemistry of the free troposphere (from the top of the boundary layer to the tropopause), is important because it contains most of the matter in the atmosphere and most of its transport and is the source of many trace gases in the boundary layer under unpolluted conditions. Many pollutants are longer lived (O_3) or more reactive (NO_2) in the free troposphere than in the boundary layer because of the lack of dry deposition and the colder temperatures. The colder temperatures also mean that trace gases in the free troposphere can have a significant greenhouse effect, whereas they have no effect in the boundary layer. Although the free troposphere can be sampled by large tethered balloons, regular measurements of trace gases other than O_3 by sondes only started in the 1980s, after the deployment of instruments on research aircraft, such as the United Kingdom Met Office's Hercules. In modern integrated airborne campaigns in the free troposphere, a comprehensive mixture of techniques is used. For example, in the airborne Pacific Exloratory Mission West (*67*), 4 gases were measured by in situ spectroscopy, 1 by remote spectroscopy, 13 by in situ chemistry, and 25 by storage of gas samples and later GC analysis. Fifteen elements and ions were also measured by filtering with later analysis. However, because of the cost of pressurized aircraft, future apparatus may more often be mounted on small unpressurized aircraft and on unmanned remotely piloted aircraft. Unmanned aircraft could rapidly change the breadth of measurement opportunities, as discussed below.

Finally, there have been few tropospheric chemistry measurements in the unpolluted Southern Hemisphere, particularly Antarctica, where models should be easiest to test because of the relatively small amounts of pollution. In the Arctic boundary layer, a rapid unexplained disappearance of O_3 has been observed in the spring, with a simultaneous increase in BrO. Theories range

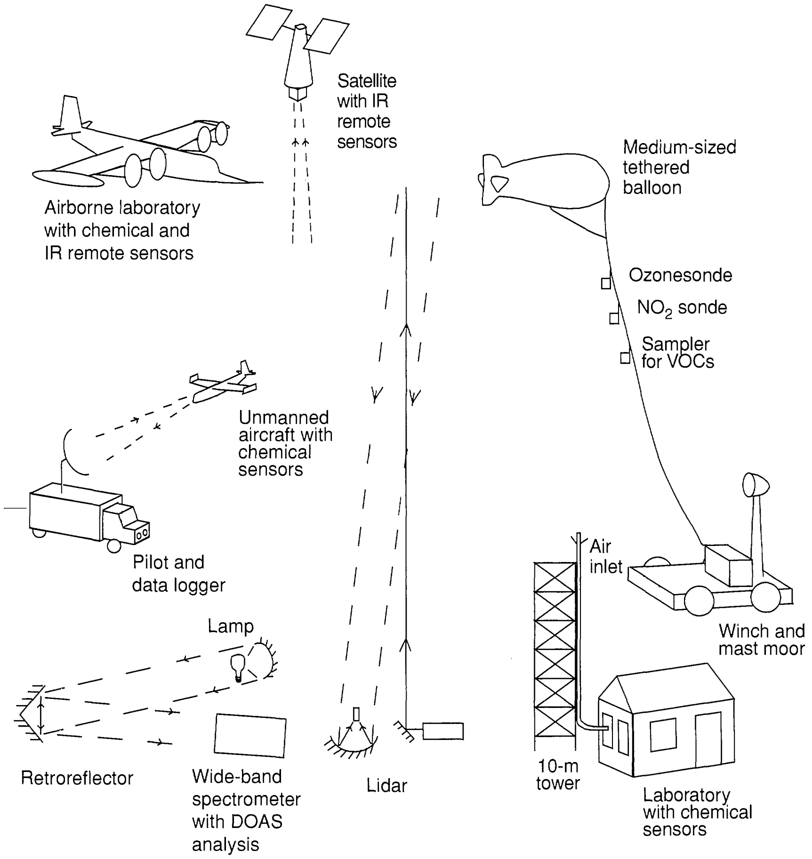

Fig. 3. Some of the platforms and sensors for present and future measurements of tropospheric trace gases.

from biological activity to sea spray, and this fascinating problem will doubtless be pursued vigorously.

Future Instruments

Currently, the range of spectroscopic techniques is broadly categorized by wavelength: DOAS in the UV and visible, using array detectors; TDL in the near- and mid-IR, sometimes with frequency modulation providing DOAS filtering; and FTS in the mid-IR. These wavelength boundaries between the techniques should blur as IR detector arrays become available and as more instruments at visible wavelengths use an FTS. Sources should also become less differentiated as the bandwidth of IR solid-state lasers becomes wider or more tunable and as they require less cryogenic cooling.

Future spectroscopic measurements will likely be dominated by wide-band systems with DOAS analysis or line-by-line correlation in the computer. Narrow-band specific instruments may only be used for tactical reasons. Recent examples are a 2-kg IR gas analyzer developed in the United Kingdom for measurements of CO_2 and H_2O from small tethered balloons, which needed extreme miniaturization; and a new CO_2 sensor with an electrically tunable Fabry-Perot etalon, which needed excellent wavelength stability over a wide temperature range. Satellite instruments are also an exception because of their long development time. For example, measurements of pollution in the troposphere (MOPITT) will use a gas-correlation cell to measure CO from NASA's AM-1 satellite in 1998. But even satellite instruments are becoming comprehensive; the tropospheric emission sensor (TES), to be launched in 2002, will measure spectra from 2.3 to 16.7 μm, generating profiles of O_3, CO, NO, NO_2, HNO_3, and other trace gases. Very recent spectra from its airborne predecessor illustrate the excellent quality of the data we may expect from TES (*68*).

Although problems with xenon white-light sources render similarly comprehensive lidar measurements impossible now, future work should reduce the pulse length and arc size of these xenon flash lamps. An exciting alternative would be a tunable femtosecond laser with a short burst of pulses; each burst would have an inherently smooth spectrum of medium bandwidth, which could then be extended by sweep-tuning during successive bursts. Meanwhile, more selective lidars that measure O_3 by the DOAS principle are already feasible (*31*); SO_2 and hydrocarbons may soon be added (*69*). This move to DOAS analysis and broad bandwidth is set to revolutionize tropospheric lidar measurements.

In the free troposphere, the population of peroxy radicals is expected to be dominated by HO_2 and CH_3O_2, so that interpretation of airborne measurements with chemical amplifiers should be more straightforward than in the polluted boundary layer, where the higher peroxy radicals interfere to uncertain degrees. Concerted laboratory and field measurements and modeling studies that address these interference problems are urgently required. For this reason, other methods that are insensitive to higher peroxy radicals should be investigated; for example, peroxy radicals could be converted to OH by reaction with O_2 and NO, and the OH could be detected with FAGE; if O_2 and NO were introduced before the expansion nozzle, the reaction would proceed more rapidly than at the reduced pressure after the nozzle.

HONO is a minor but important component of total reactive nitrogen that cannot easily be measured by a chemical technique. Chemical measurement of HONO is important in its own right and for actinometric measurements of *j*(HONO). A possible approach would be conversion of the OH and H photoproducts to HO_2 radicals, with detection of HO_2 by a chemical amplifier. A similar innovative approach to actinometric measurements of *j*(HCHO) would be to measure the H and HCO products after oxidation to HO_2; alternatively, UV resonance fluorescence might be used to measure CO for the CO + H_2 channel. Similarly innovative detection systems borrowed from traditionally separate instrumentation could be used with gas chromatographs; for example, using an IR FTS to further analyze the products. In this way, we feel that there could well be a significant synthesis of chemical techniques for future tropospheric measurements as emphasized in Fig. 4.

Miniaturization may dramatically influence instrument development, with an emphasis on solid-state chemical sensors (a sensor for O_3 is under active development, and others are at the design stage), on sampling for GC analysis without cryogens, and on miniaturization of FTSs. Some innovative ideas for miniaturization of an FTS have recently been developed, involving simpler optical components such as a birefringent prism to split the paths and a single lens to combine them (*70*); and involving the recording of all the fringes on an array detector, rather than just the central fringe of the Newton's ring pattern, to avoid moving parts (*71*). Such exciting developments may render narrow-band measurements totally redundant. Miniaturization will be driven by the demands of the future platforms discussed above (medium-sized balloons, small and unmanned aircraft, and measurements in Antarctica); each requires smaller, lightweight, lower-power apparatus that is self-contained. This will be the major challenge in instrument development for tropospheric chemistry during the next decade.

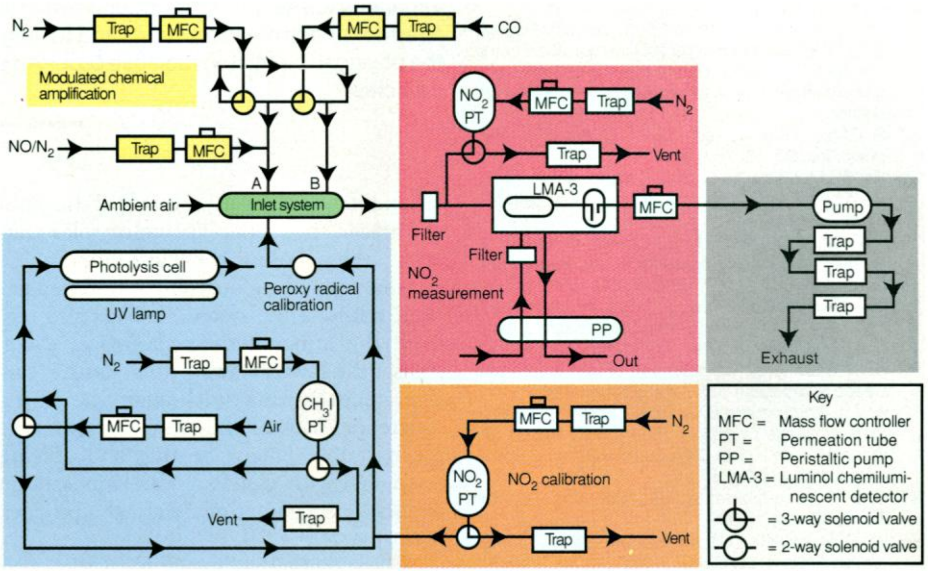

Fig. 4. Schematic diagram of a peroxy radical chemical amplifier. Like many modern chemical instruments, this consists of several subsystems, which are identified in the figure: an inlet system, a system for NO_2 measurement, a system for NO_2 calibration, a system for peroxy radical calibration using a source of CH_3O_2 radicals based on CH_3I photooxidation, and a system for exhaust gas treatment. The data acquisition system is not shown. During deployment in field studies, the inlet system is mounted on a tower and the other equipment is housed in the laboratory. The instrument is operated in one of three modes: ambient measurements, NO_2 calibration, or peroxy radical calibration. To improve the detection limit or to enlarge the range of gases measured, future chemical instruments are likely to exchange subsystems such as those shown here with subsystems currently used in other types of chemical instruments.

REFERENCES AND NOTES

1. D. L. Albritton, F. C. Fehsenfeld, A. F. Tuck, *Science* **250**, 75 (1990).
2. U. Platt, in *Air Monitoring by Spectroscopic Techniques, Chemical Analysis Series 127* (Wiley, New York, 1994), chap. 2.
3. R. D. Bojkov, *J. Clim. Appl. Meteorol.* **25**, 343 (1986).
4. E. Fonrobert, in *Chemie in Einzeldarstellungen* (Ferdinand Enke, Germany, 1916), vol. 9.
5. R. J. Strutt, *Proc. R. Soc. London A*, **94**, 260 (1918).
6. D. Chalonge and E. Vassy, *Rev. Opt.* **4**, 113 (1934).
7. A. Adel, *Astrophys. J.* **93**, 509 (1941).
8. M. V. Migeotte, *ibid.* **107**, 400 (1948).
9. A. Adel, *ibid.* **94**, 451 (1941).
10. M. V. Migeotte, *Phys. Rev.* **75**, 1108 (1949).
11. A. Adel, *ibid.*, p. 1766.
12. H. G. Reichle Jr. and H. A. Wallio, *J. Geophys. Res.* **91**, 9841 (1986); H. G. Reichle Jr. *et al.*, *ibid.* **95**, 9845 (1990).
13. M. Migeotte, L. Neven, J. Swenson, *Mem. Soc. R. Sci. Liege Spec. 1* (1956).
14. D. H. Ehhalt, U. Schmidt, R. Zander, P. Demoulin, C. P. Rinsland, *J. Geophys. Res.* **96**, 4985 (1991).
15. G. H. Mount, *ibid.* **97**, 2427 (1992).
16. D. Perner *et al.*, *Geophys. Res. Lett.* **3**, 466 (1976).
17. G. Hübler, D. Perner, U. Platt, A. Tönnissen, D. H. Ehhalt, *J. Geophys. Res.* **89**, 1309 (1984).
18. U. Platt, D. Perner, H. W. Pätz, *ibid.* **84**, 6329 (1979).
19. U. Platt and D. Perner, *Geophys. Res. Lett.* **7**, 89 (1980).
20. J. F. Noxon, R. B. Norton, E. Marovich, *ibid.*, p. 125.
21. H.-P. Dorn, U. Brandenberger, T. Brauers, M. Hausmann, D. H. Ehhalt, *ibid.* **23**, 2537 (1996).
22. H. K. Roscoe, D. J. Fish, R. L. Jones, *Appl. Opt.* **35**, 427 (1996).
23. J. P. Pommereau, in *Proceedings of the EUROTRAC Symposium 1990*, P. Borrell, Ed. (SPB Academic Publishing, The Hague, Netherlands, 1991), pp. 467–468.
24. A similar approach of wide bandwidth with an array detector was taken by J. M. C. Plane and C-F. Nien [*Rev. Sci. Instrum.* **63**, 1867 (1992)], who included the bands of NO_3.
25. E. Murray, in *Handbook of Air Pollution Analysis*, R. Perry and R. J. Young, Eds. (Chapman & Hall, London, 1977), chap. 8.
26. Unlike conventional lidar, the purpose of the time-of-flight information in this particular application of the Stanford lidar was to ensure that the chosen topographic target was observed and so the path length defined.
27. B. Galle, L. Klemedtsson, D. W. T. Griffith, *J. Geophys. Res.* **99**, 16575 (1994).
28. W. W. McMillan, L. L. Strow, W. L. Smith, H. E. Revercomb, H. L. Huang, *Geophys. Res. Lett.* **23**, 3199 (1996).
29. J. Pelon, P. Flamant, M. L. Chanin, G. Megie, in *Proceedings of the Quadrennial Ozone Symposium*, J. London, Ed. (IAMAP, Boulder, CO 1981), p. 130.
30. E. V. Browell, A. F. Carter, S. T. Shipley, in *Proceedings of the Quadrennial Ozone Symposium*, J. London, Ed. (IAMAP, Boulder, CO, (1981), pp. 99–107.
31. A. M. South *et al.*, abstract 416 of the Quadrennial Ozone Symposium book of abstracts (1996).
32. A. Volz-Thomas and B. A. Ridley, *Scientific Assessment of Ozone Depletion: 1994* (WMO Report 37, World Meteorological Organization, Geneva, Switzerland, 1995), chap. 5.
33. C. E. Canosa-Mas *et al.*, *J. Chem. Soc. Faraday Trans.* **92**, 2211 (1996).
34. W. R. Stockwell, J. B. Milford, D. Gao, Y-J. Yang, *Atmos. Environ.* **29A**, 1591 (1995).
35. A. C. Lewis, P. W. Seakins, A. M. Denha, K. D. Bartle, M. J. Pilling, *ibid.*, p. 1871.
36. S. A. Penkett *et al.*, *J. Geophys. Res.* **98**, 2865 (1993).
37. G. J. Wendel, D. H. Stedman, C. A. Cantrell, L. Danrauer, *Anal. Chem.* **55**, 937 (1983).
38. Two molecules of NO_2 are believed to be involved [C. A. Cantrell *et al.*, *J. Geophys. Res.* **98**, 2897 (1993)].
39. T. J. Kelly, C. W. Spicer, G. F. Ward, *Atmos. Environ.* **24A**, 2397 (1990).
40. H. I. Schiff, D. Pepper, B. A. Ridley, *J. Geophys. Res.* **84**, 7895 (1979).
41. F. C. Fehsenfeld *et al.*, *ibid.* **92**, 14710 (1987).
42. M. McFarland *et al.*, *ibid.* **91**, 5421 (1986).
43. M. J. Bollinger, R. E. Sievers, D. W. Fahey, F. C. Fehsenfeld, *Anal. Chem.* **55**, 1980 (1983).
44. D. W. Fahey, C. S. Eubank, G. Hubler, F. C. Fehsenfeld, *J. Atmos. Chem.* **3**, 435 (1985).
45. D. R. Crosley, *J. Geophys. Res.* **101**, 2049 (1996).
46. C. A. Cantrell and D. H. Stedman, *Geophys. Res. Lett.* **9**, 846 (1982).
47. D. R. Hastie, M. Weissenmayer, J. P. Burrows, G. W. Harris, *Anal. Chem.* **63**, 2048 (1991).
48. D. Mihelcic and A. Volz-Tomas, in *Proceedings of the EUROTRAC Symposium*, P. Borrell, P. M. Borrell, W. Seiler, Eds. (SPB Academic Publishing, The Hague, Netherlands, 1994), pp. 379–383.
49. A. Volz-Thomas *et al.*, in *Proceedings of the EUROTRAC Symposium*, P. M. Borrell, P. Borrell, T. Cvitas, K. Kelly, W. Seiler, Eds. (SPB Academic Publishing, The Hague, Netherlands, 1996), pp. 621–626.
50. H. E. Heitlinger *et al.*, in press.
51. D. Mihelcic, P. Muesgen, D H Ehhalt, *J. Atmos. Chem.* **3**, 341 (1985).
52. D. Mihelcic, D. Klemp, P. Muesgen, H. W. Paetz, A. Volz-Thomas, *ibid.* **16**, 313 (1993).
53. T. M. Hard, R. J. O'Brien, C. Y. Chan, A. A. Merhrabzadeh, *Environ. Sci. Technol.* **18**, 768 (1984).
54. G. H. Mount and F. L. Eisele, *Science* **256**, 1187 (1992).
55. T. Brauers *et al.*, *Geophys. Res. Lett.* **23**, 2545 (1996).
56. M. K. Dubey, T. F. Hanisco, P. O. Wennberg, J. G. Anderson, *ibid.*, p. 3215.
57. F. L. Eisele *et al.*, *J. Geophys. Res.* **99**, 18605 (1994).
58. D. J. Tanner and F. L. Eisele, *ibid.* **100**, 2883 (1995).
59. C. A. Cantrell, R. E. Shetter, D. J. Tanner, F. L. Eisele, *Eos Trans.* **77**, 46 (1996).
60. T. Reiner, M. Hanke, F. Arnold, *J. Geophys. Res.* **102**, 1311 (1997).
61. A. A. Viggiano, *Mass Spectrom. Rev.* **12**, 115 (1993).
62. R. E. Shetter, A. H. McDaniel, C. A. Cantrell, S. Madronich, J. G. Calvert, *J. Geophys. Res.* **97**, 10349 (1992).
63. K. O. Lantz, R. E. Shetter, C. A. Cantrell, S. J. Flocke, J. G. Calvert, S. Madronich, *ibid.* **101**, 14613 (1996).
64. W. Junkermann, U. Platt, A. Volz, *J. Atmos. Chem.* **8**, 203 (1989).
65. A. Volz-Thomas *et al.*, *J. Geophys. Res.* **101**, 18613 (1996).
66. G. Baumbach and U. Vogt, *EUROTRAC Newsl.* **16**, 23 (1995).
67. J. M. Hoell *et al.*, *J. Geophys. Res.* **101**, 1641 (1996).
68. H. Worden, R. Beer, C. P. Rinsland, *ibid.* **102**, 1287 (1997).
69. R. L. Jones, personal communication.
70. S. Kawata, Y. Inouye, S. Minami, *SPIE* **1145**, 567 (1989).
71. J. Linkeman, F. Romero-Borja, H. O. Tittel, *ibid.* **1575**, 184 (1991).
72. J. E. Lovelock, R. J. Maggs, R. J. Wade, *Nature* **241**, 194 (1973).
73. W. Schrimpf, K. P. Muller, F. J. Johnen, K. Lienaerts, J. Rudolph, *J. Atmos. Chem.* **22**, 303 (1995).
74. E. Atlas, W. Pollock, J. Greenberg, L. Heidt, A. M. Thompson, *J. Geophys. Res.* **98**, 16933 (1993).
75. We thank R. L. Jones, D. J. Fish, R. A. Cox, P. E. Morris, D. A. Peel, and an anonymous referee for helpful discussions and comment.

Cloud Microphysics and Climate

M. B. Baker

Recent studies have shown that global radiative and hydrological fluxes are strongly linked to microphysical processes in clouds. The sensitivity of predictions of climate variations to assumptions about the microphysical processes has led to new approaches to atmospheric measurements and to heightened interest and progress in understanding the physical chemistry, radiative properties, and kinetics of small solid and liquid aqueous particles.

Clouds cover almost two thirds of the global surface. They reflect incoming solar radiation, thus cooling the Earth-atmosphere system, and reduce outgoing infrared radiation, warming the system. Clouds also regulate the atmospheric hydrological cycle, transporting water away from Earth's surface, redistributing it through the atmosphere and back to the surface by means of precipitation. Latent heating and cooling associated with clouds modify atmospheric circulations, and thunderclouds produce lightning.

All of these phenomena have their origins in cloud microphysical processes, that is, processes involving ice and liquid-water particles whose dimensions range from under a micrometer to a few millimeters. Changes in cloud microphysical processes can modify the spatial extent, spatial distribution, and lifetimes of clouds, the water vapor distribution outside of clouds, and the fluxes of water and radiation through the atmosphere. This article focuses on the resulting changes in the distribution of atmospheric water and in the radiative fluxes at the top of the atmosphere (TOA). The discussion is centered on the following illustrative issues: possible modification of TOA radiative fluxes by anthropogenic aerosol particles in clouds, the impacts of ice particles on the TOA radiative fluxes, and the roles of cloud microphysical processes in regulating the atmospheric hydrological cycle.

The links between cloud microphysical parameters and the TOA radiative fluxes can be understood from a brief summary of Earth's radiation budget. The incoming TOA flux of solar radiation is about 340 W/m^2 on a global, annual average and is concentrated at short wavelengths ($\lambda \leq 4$ μm). About 30% of this energy is reflected

---

The author is in the Geophysics Program and Atmospheric Sciences Department, University of Washington, Seattle, WA 98195, USA.